JOURNAL OF MATERIALS SCIENCE 24 (1989) 2177–2182

Al–Si substitution in α-phase AlMnSi

J. E. TIBBALLS*
Senter for Industriforskning, PB 124, Blindern, N-0314 Oslo 3, Norway
R. L. DAVIS
Australian Institute for Nuclear Science and Engineering, Locked Bag, Menai, NSW, Australia
B. A. PARKER
Department of Materials Engineering, Monash University, Clayton, Victoria, Australia

The α-phase of the Al–Mn–Si ternary system has been precipitated from four liquid solutions (2.8 wt% Mn–3.7 wt% Si, 4.5 wt% Mn–7 wt% Si, 7.7 wt% Mn–10 wt% Si and 8.7 wt% Mn–12.6 wt% Si) and equilibrated slightly over the melting point of the (secondary) solid solution. Quenching into water enabled the precipitates to be separated from the solid solution and the co-nodal tie-lines for the α-phase and liquid to be determined. The silicon content varied from 9.8 to 11.8 wt%, while the manganese content, 29.6 ± 0.6 wt%, did not vary significantly. The lattice parameter of the cubic unit cell decreased from 1.267 6(2) nm to 1.265 10(4) nm with increasing silicon. Neutron powder diffraction showed silicon to constitute approximately 50% of atoms on the icosahedral aluminium sublattices and 70% of a six-fold aluminium site in the interstices between the almost spherical, 54-atom clusters. This decrease in unit cell volume is interpreted as evidence for substitution of the silicon atoms on the six-fold sublattice.

1. Introduction

The ductility of AA 3000-series aluminium alloys, including the highly formable canstock alloys [1] is due largely to the presence of a fine distribution of the phase α-AlMnSi. The precipitation of this phase rather than other, less advantageous, ones is controlled by the level of silicon in solid solution after casting. This depends in turn on the melt composition and the silicon content of phases precipitated during casting. The silicon content of the α-phase found in untreated cast alloys has been reported as varying between 5 and 13 wt % Si, with the lowest percentages when iron has replaced more than 80% of the manganese [2]. Precise process control by accounting for silicon requires a detailed knowledge of the thermodynamic equilibria into which the phase enters, as well as the rate-determining kinetics.

The crystal structure of the α-AlMnSi phase [3] can be described in terms of clusters of 54 atoms around vacant sites at the origin and body-centre positions. An icosaedron of aluminium atoms at a radius of 0.243 nm constitutes the inner shell of each cluster. The outer shell consists of an icosahedron of manganese atoms at 0.475 nm, along the same radii as the inner-shell atoms and aluminium atoms on two crystallographic sublattices that form the 30 vertices of an almost regular icosidodecahedron. The dimensions of the clusters at the origin and the centre differ by about 1%. Neighbouring clusters are linked by the octahedral packing between aluminium atoms in their outer shells and, in the interstices, by twelve tetrahedra of aluminium atoms containing a central atom. In the low symmetry structure, the configurations of the tetrahedra are ordered; in the body-centred structure they are disordered.

In a recent development, the α-AlMnSi phase has been suggested [4] to be the stable crystalline compound having the icosahedral atomic arrangement which forms the basic structural unit of the apparently quasicrystalline phases Al_mM where M is a transition element manganese, iron or chromium. The value of m has been determined as approximately 4 [5]. Furthermore, the icosahedral basis vector for the icosahedral symmetric unit which corresponds to radial dimension to the manganese atoms has been estimated as 0.460 nm [6].

Despite the annual production of approximately 100 000 tonnes of this phase in canstock and the scientific interest in quasicrystalline phases, there exists little data on equilibria involving the α-phase. The classical studies [7–10] were all undertaken on samples solidified at a variety of continuous cooling rates. Pratt and Raynor [10], who examined the phase extracted from melts cooled at 45° Ch^{-1}, found a range of compositions (see Fig. 1) but cite no initial or residual melt compositions from which equilibria might be determined. Phragmen's [9] work states initial melt and phase compositions but does not specify details of cooling rates.

The data required to uniquely specify a thermodynamic equilibrium in a three-component system are the compositions of the coexisting phases and the temperature. Furthermore, in order to model the composition dependence of the Gibbs energy of the phase

*Author to whom all correspondence should be addressed.

0022–2461/89 $03.00 + .12

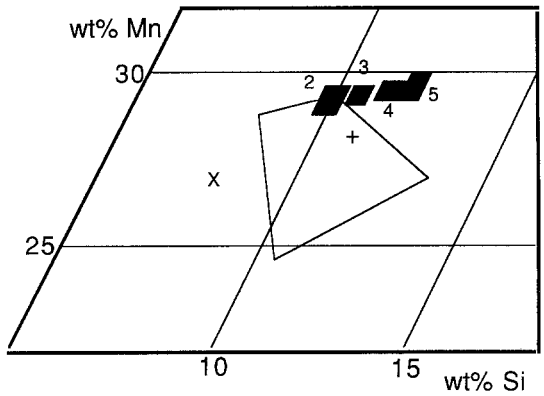

Figure 1 Compositions of α-AlMnSi specimens. Filled rhombohedra present study; (+) X-ray single-crystal sample [9]; (x) Phragmen's analysis of precipitate from 4 wt % Mn–4 wt % Si; open quadrilateral, boundaries of Pratt and Raynor's [8] range of homogeneity.

[11], it is necessary to know whether the variable composition is due to the incorporation of vacancies or to atomic substitution on one or more crystal sublattices. The present study is designed to obtain the equilibrium data, to decide between atom or vacancy substitution and to determine the sublattices on which silicon resides.

2. Sample preparation

Four melts with the compositions given in Table I were prepared for 99.995% Mn, 99.999% Si and 99.995% Al by melting approximately 60 g mixtures at 950° C in Al_2O_3 crucibles. The concentrations were chosen to maximize the production of the primary α-phase for a given silicon content. Each crucible was sealed in quartz glass ampoules under a reduced pressure of argon.

After cooling quickly to a temperature, T_A, near the liquidus temperature of each melt [12], cooling continued at a rate of 3° C h^{-1} to a temperature, T_B, just above the melting point of the expected residual phase. The crucible was then held at $T_B \pm 3°$ C for 25 to 30 h and quenched by breaking the ampoule under water.

The primary α-phase was visible as bright, 0.5 to 1 mm crystals accumulated at the base of the ingots. Approximate 5 g pieces were cut and the aluminium solid solution dissolved [13]. The large α-phase crystals were held together by a friable microstructure of interdendritic precipitates. Specimens for diffraction experiments were separated by means of an ultrasound bath and a 0.5 mm mesh sieve.

3. Analysis

Polished cross-sections containing several large crystals were analysed using a Cameca electron microprobe in wavelength dispersive mode. The results of the analyses are given in Table I. For casting 2, the holding temperature T_B lay in the three-phase, liquid–aluminium solid solution–α-AlMnSi region. Analyses of the 600 μm secondary aluminium dendrites that grew at T_B and the 22 μm dendrites that formed during quenching, were identical within error.

The microprobe analyses were compared with wet chemical analyses of α-phase extracted from casting 2. This gave 29.2 ± 0.2 wt % Mn, 61.8 ± 0.4 wt % Al, silicon not being analysed because of the difficulty of retaining silanes produced on dissolving the α-phase in HF. The remainder, 9.0 ± 0.6 wt % Si, is lower than the microprobe analysis because of aluminium solid solution enclosed in the α-phase grains and therefore not dissolved in the initial extraction. X-ray diffraction of sample 2 showed very weak aluminium lines which confirmed this interpretation (See Fig. 2.)

The concentrations of the residual liquid were estimated from area analyses of the dendrite and the interdendritic region. Three estimates of the relative proportions of each region were obtained by 100 μm × 100 μm area analyses using a Jeol 826 scanning electron microscope and analytical energy dispersive X-ray spectrometry (EDS); quantitative analysis of optical images and, where applicable, the lever rule applied to the α-phase and initial melt compositions. The last gave the most precise determination of silicon but all three methods agreed.

The compositions of the initial mixtures, the residual melt and α-phase crystals are given for the four castings in Table I.

4. X-ray diffraction

Diffractograms for each sample were obtained on a Rigaku automatic diffractometer from powders prepared by crushing selected crystals. Using filtered Cu$K\alpha$ radiation, each specimen was scanned continuously from 15° to 150° in 2θ at 0.15° min^{-1} and sampled at 0.02° intervals. The data were smoothed using a five-point procedure and the $K\alpha_2$ peak stripped by a modified Rachinger method. The unit cell dimension, a_0, quoted in Table I was estimated by extrapolating to $\cos^2\theta\,[(\sin\theta)^{-1} + \theta^{-1}] = 0$ the a_0 values calculated for 12 strong peaks with $34 < h^2 + k^2 + l^2 < 230$. (Identification of reflections for $h^2 + k^2 + l^2 < 100$ was checked against the Powder Diffraction

TABLE I Compositions of the initial mixtures, residual melts and α-AlMnSi precipitates; cooling ranges and holding temperatures and α-phase unit cell dimensions from four experiments. Estimated standard deviations in the last quoted figure(s) given in brackets

Casting no.	Temperature (° C)		Initial mixture		Composition (wt %)				Unit cell, a_0 (nm)
	T_A	T_B	Mn	Si	Residual melt		α-AlMnSi		
					Mn	Si	Mn	Si	
2	675	620	2.80	3.74	1.07(8)*	6.3(3)	29.2(4)	9.8(3)	1.2676(2)
3	730	635	4.43	7.08	0.80(8)	6.6(1)	29.5(2)	10.5(3)	1.26666(10)
4	760	650	6.67	10.00	1.0(1)	9.7(2)	29.6(2)	11.3(3)	1.26601(14)
5	775	650	8.66	12.60	0.82(8)	12.9(2)	29.7(3)	11.8(3)	1.26510(4)

*A co-existing third phase, the solid solution of manganese and silicon in aluminium, was analysed as 0.53(6) wt % Mn–0.75(5) wt % Si.

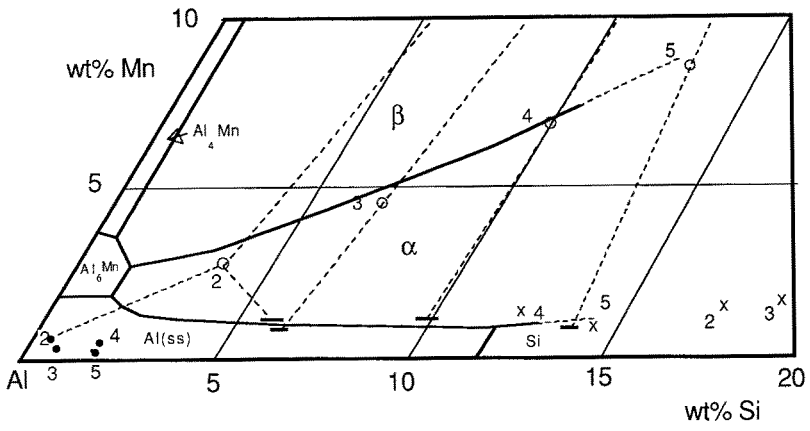

Figure 2 (○) Analyses of the initial mixtures, (——) residual melt, (●) dendrites and (x) interdendritic spaces for castings 2 to 5. Liquidus boundaries from [7] are indicated.

File 6-0669 which incorrectly designates the phase as $Mn_{12}Si_7Al_5$ rather than $Al_{50}Mn_{12}Si_7$. We would suggest the phase is a member of a solid solution whose end-members can be denoted $Al_{17}Mn_4Si_2$ and $Al_{16}Mn_4Si_3$.) Several reflections with odd values of $h^2 + k^2 + l^2$ (notably 29, 43, 69 and 77) were detected, indicating the space group Pm3 rather than Im3 [14].

The variation of unit cell volume with silicon concentration of the α-phase is shown in Fig. 3.

5. Neutron diffraction

A 6.6 g sample of the α-phase extracted from casting 5 was mounted on the high-resolution powder diffractometer at the HIFAR research reactor and a diffractogram collected with 0.189 nm wavelength neutrons. The diffractogram was analysed by the Rietveld [15] method to obtain apparent occupancies of the nine aluminium sublattices in the crystal structure [3]. Scattering lengths of aluminium and silicon were taken as 0.3449 and 0.4149 nm, respectively, and for manganese −0.373 nm. Initially, occupations were refined individually together with two isotropic thermal parameters, one for the manganese and one for the aluminium sublattices, and parameters describing peak and background shape [16]. This analysis showed that six sublattices comprising 84 atomic sites in the unit cell had occupancies of 98 ± 3% Al and three sublattices had apparent aluminium occupancies significantly greater than 100%.

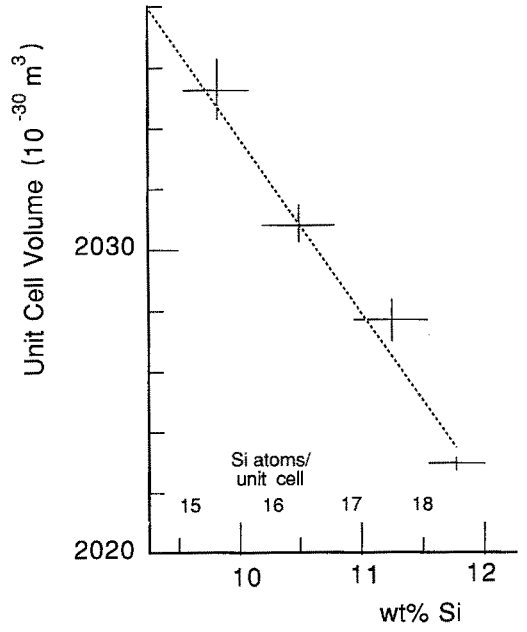

Figure 3 Variation of the unit-cell volume of α-AlMnSi as a function of silicon content.

Attempts to refine individual thermal parameters revealed that they were highly correlated with the occupancies. The six 98% Al sublattices were, therefore, assigned equal occupancies and refinement continued with B parameters refined individually for the following sets of sublattices: B_1 for Al_1, Al_8, Al_2 and Al_9, which constitute the aluminium sites in the outer shells; B_2 for Al_6 and Al_7, which make up the interstitial tetrahedra; B_3 for Al_3 which is in the middle of these tetrahedra; and B_4 for Al_4 and Al_5 which are the inner shell, icosahedral sublattices. B_0 denotes the thermal parameter for Mn_1 and Mn_2.

The final weighted *R* factor was 4.06% and the goodness-of-fit 1.31. Much of the residual arose from weak peaks from silicon which had formed on solidification of the residual melt in the interstices of the α-phase crystals.

The total apparent aluminium occupancy of the sublattices was 101%, c.f. 103.2% expected for 18 silicon atoms/unit cell as found by analysis. If this average 98% occupancy applies equally to all sublattices, the fractions of silicon on each sublattice become those shown in Table II. The Al_6 sublattice consistently showed the highest occupancy of the six sublattices with less than 100% apparent aluminium.

6. Discussion

The compositions shown for the residual melts are reasonably consistent with the published phase diagram [7, 12], the major liquidus boundaries of which are indicated in Fig. 2. Variations in quenching rates

TABLE II Occupancy and thermal parameters for manganese and aluminium sublattices in α-AlMnSi from neutron diffraction

Sublattice	Apparent occupancy	Fraction Si	Thermal parameter
$Mn_1 + Mn_2$	1 (fixed)	–	B_0 0.64(6)
Al_1	0.96(5)	0	B_1 0.79(5)
Al_2	0.97(5)	0	
Al_3	1.12(4)	0.69(19)	B_3 0.55(7)
Al_4	1.09(4)	0.55(15)	B_4 0.35(7)
Al_5	1.06(4)	0.42(15)	
Al_6	0.99(3)	0.08(10)	B_2 0.63(7)
Al_7	0.99(4)	0.06(10)	
Al_8	0.98(3)	0	B_1 0.79(5)
Al_9	0.98(3)	0	

and differences in cooling rates between the present investigation ($3°C\,h^{-1}$) and the original data (8 to $10°C\,min^{-1}$) [7] account for the differences. At the cooling rates of the original study [7] it would appear that undercooling of up to 15° C is needed to nucleate the α-phase which is a reflection of its complex crystal structure.

The variations in manganese content found [8] in solidification products can be due to growth conditions in the interdendritic spaces of solidifying alloys. Preliminary high-resolution TEM investigations [17] indicate high densities of planar defects in the solidification products.

The observed variation in silicon content in samples 2 to 5 may be due to substitution on one or more sublattices or be uniformly distributed. Comparison of the original single-crystal structure [3] with the variations in unit-cell volume suggest that one sublattice is favoured. We note first that the single crystal data apply to a structure with 16.5 Si atoms per unit cell and then examine the effect of silicon for aluminium substitution on sites in the Al_3 and Al_4 or Al_5 sublattices.

The Al_3 site has an approximately icosahedral arrangement in its first co-ordination shell but two manganese atoms in the shell allow only one mirror plane. The average distance to the aluminium atoms is 0.2796 nm which, if the variation in silicon content is confined to this sublattice, would have had 45% Si (cf. 70% in sample 5). Simple Goldschmidt radii considerations require the silicon atom to have a radius of 0.129 nm (cf. Al, 0.143 nm). If the two-fold site is occupied by silicon atoms, averaged bond lengths can be consistently described by the atomic radii for aluminium, manganese and silicon given in Table III. In highly co-ordinated structures with widely varying bond lengths, the cubes of these averaged radii provide measures of the relative atomic volumes for the structure. Taking atomic volume to be proportional to the cube of the atomic diameter and the atomic volume of aluminium as $0.0166\,nm^3$ the unit cell volume is reduced by $4 \times 10^{-3}\,nm^3$/silicon for aluminium substitution.

The alternative, that silicon substitutes on the Al_4 or Al_5 sublattices, requires a more complex analysis because of the neighbouring vacant site. The interatomic distances between the icosahedral sites are extremely short, indicating compression. The compression is confirmed by the small thermal parameter B_4 found by neutron diffraction for these sublattices. The correspondingly long distances between atoms in the outer shell suggests that the 54-atom cluster is indeed a structural unit for which the total volume change on silicon for aluminium substitution must be calculated. The volume of an icosahedron is related to the radius of its circumsphere by

$$\begin{aligned} V &= (4/3)\phi R^3 \\ &= 2.536R^3 \\ \phi &= 5^{1/4}[(5^{1/2} + 1)/2]^{1/2} \end{aligned}$$

The circumradius R_2 of the outer (manganese) icosahedron is given by

$$\begin{aligned} R_2 &= R_1 + d \\ &= (1 + \phi)[fd_{Si} + (1 - f)d_{Al}] + d \end{aligned}$$

where R_1, the circumradius of the inner icosahedron, is proportional to the average interatomic spacing $[fd_{Si} + (1 - f)d_{Al}]$ and d is the Al–Mn spacing between the inner and outer icosahedra for a silicon fraction $f = 0$. The observed variation in unit cell volume of -3.7×10^{-3} nm/silicon for aluminium substitution is consistent with a difference in atomic diameters for the two atoms of only 0.012 nm. The atomic radii derived for silicon and aluminium respectively are given in Table III. Do such small aluminium diameters occur in intermetallics of transition metals with aluminium and silicon?

The compound nearest in composition is β-$Al_{10-x}Mn_3Si_x$ for which Robinson [18] gives detailed lattice parameter–composition data and Taylor [19] produced the metastable end-member $Al_{10}Mn$. As shown in Fig. 4, the unit cell volume decreases by $6 \times 10^{-3}\,nm^3$ per silicon for aluminium substitution.

As with the α-phase, β-AlMnSi shows no significant variation in manganese content when precipitated from slowly cooling melts of varying composition. Furthermore, like α the silicon content of the β-phase is directly correlated with that of the melt [18]. Only when the silicon analysis corresponds to $x > 1$ does the manganese content decrease slightly but the crystal habit and mechanical properties reported for this sample suggest a significant density of growth faults. The silicon atoms have been variously allocated to a two-fold sublattice [18], a twelve-fold sublattice shared with aluminium [19] and a six-fold sublattice shared with manganese when zinc is added to the

TABLE III Volume changes and apparent atomic diameters (AAD) for silicon and aluminium substitution in α- and β-AlMnSi and β-Mn and α-Al

Phase	Substitution sublattice	AAD (nm)			ΔV ($10^{-3}\,nm^3\,atom^{-1}$)
		Al	Mn	Si	
α-AlMnSi	6(f) [Al_3]	0.141	0.120	0.130	−3.7
	12(j) [Al_4] or 12(k) [Al_5]	0.132		0.126	
β-AlMnSi	2(d)	0.143	0.125	0.125	−6.0
β Mn(Al)		0.137	0.129		+2.2
β Mn(Si)			0.129	0.129	−0.1
α Al(Mn)	4(a)	0.143	0.130		−4.1
α Al(Si)	4(a)	0.143		0.137	−2.2

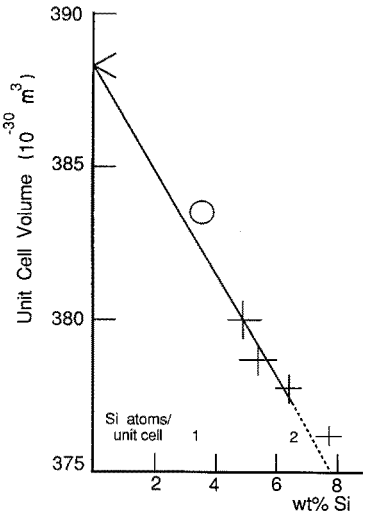

Figure 4 Variation of the unit cell volume of β-AlMnSi as a function of silicon content. (+) From [14]; (<) [15]; (○) [16] for zinc-containing phase.

phase [20]. None of these allocations is supported by conclusive arguments. We offer additional arguments based on the unit cell volume change for the two-fold sublattice being preferentially occupied by the silicon atoms as proposed originally [18]. Again taking the atomic volume of aluminium as 0.0166 nm^3, the atomic volume for silicon in the two-fold site is 0.0106 nm^3, calculated from average interatomic distances. The difference is exactly that expected from the unit cell–Si content plots (Fig. 4). Allocating the silicon atoms a 1/6th share of the twelve-fold aluminium-sublattice [19] causes the average Al–Si separation to appear greater than the Al–Al separation and the calculated change in unit-cell volume to have the wrong sign.

Lattice constant investigations of hexagonal α_H-AlFeSi [21] show cell-volume variations consistent with direct one-for-one Al ↔ Si substitution and the apparent atomic diameter (AAD) of silicon dissolved in aluminium. In Al_3Fe, on the other hand, silicon increases the cell volume by 2.7×10^{-3}/wt % Si [22] but this compound exhibits variable aluminium content in its binary form [23], so vacant aluminium lattice sites already exist to be occupied by silicon without substitution for aluminium [24].

Together these observations suggest that diameters of aluminium as small as that required for substitution of Al_4 or Al_5 do not occur and that Al_3 (and perhaps Al_6 if this sublattice has a significant fraction of silicon atoms) is the main substitution sublattice.

The investigated range of composition covers only liquid compositions for which the α-phase is the primary solidifying phase. The range is presumably larger when one includes the three-phase Al, α and Al_6Mn region and for higher concentrations of silicon in the initial melt.

Complete substitution of silicon for aluminium on the Al_3 sublattice represents a range of 3.8 wt % in silicon content and some substitution on to Al_6 and Al_7 seems likely. No change in silicon fraction on the Al_4 or Al_5 sublattices is necessary except to account for the lower ($\lesssim$ 7 wt % Si) [2, 14] found in iron-containing samples of the cubic α-phase. This suggests the silicon concentration on these sublattices is linked to the Mn/Fe ratio. Presumably the extra valence electron concentration available from silicon atoms destabilizes the vacant icosahedral sites when it cannot be accepted by the d or sd-hybrid states of the surrounding transition metal atoms.

The reduction in silicon content could also be achieved through the introduction of vacancies. The large decrease in unit cell volume (2×10^{-3} nm^3) per iron atom substituted [9, 14] can only be reconciled with the small differences in the atomic volumes usually assigned to manganese and iron if vacancies occur on the manganese or aluminium sublattices when iron is present. The difference is approximately equivalent to 4 atoms per unit cell. We note that Liu Ping and Dunlop [25] postulate a long-range ordering of four iron atom vacancies per cubic unit cell in the α_T phase.

The observed stabilization by silicon of the vacant icosahedral site at the centre of the basic, 54 atom cluster has to be accommodated by hypotheses (e.g. [4]) that it forms the structural basis of apparently five- and ten-fold symmetric quasicrystals.

7. Conclusions

Analysis of millimetre-sized particles of the α-AlMnSi phase precipitated under equilibrium conditions reveals that composition variations are restricted to aluminium and silicon concentrations. Neutron powder diffraction shows the silicon atoms to occupy approximately 50% of three crystallographic aluminium sublattices: the two icosahedra immediately surrounding the vacant lattice sites at the origin and body centre; and the six-fold sublattice of atoms in the interstices between the 0.475 nm nearly spherical 54 atom clusters centred on the vacant sites. X-ray powder diffraction measurements show that the unit cell volume decreases with increasing silicon content more rapidly than expected for one-for-one Al–Si substitution.

This observation is compared with the neighbouring β-phase and interpreted as evidence that the variation in total silicon content chiefly reflects changes in the fraction of silicon on the six-fold interstitial site. The fraction of silicon on the twelve-fold icosahedral sublattice is postulated to be determined by a total electron concentration required to stabilize the vacant site.

Acknowledgements

Sample preparation and analyses were undertaken as part of a project funded by Hydro Aluminium a.s. and the Royal Norwegian Council for Industrial Research (NTNF). One author (JET) thanks his colleagues Arid G. Andersen, Kari Baardseth and Jens-Anton Horst. The X-ray analysis was performed on facilities at the Department of Materials Engineering, Monash University, Australia, where the author held a travelling scholarship provided by the NTNF. Neutron diffraction facilities at Lucas Heights were provided by the Australian Nuclear Science and Technology Organization.

References

1. H. P. FALKENSTEIN, "The formability of aluminium sheet alloys" (Aluminium Verlag, Dusseldorf, 1983).

2. M. ARMAND, *Compt. Rend.* **235** (1952) 1506.
3. M. COOPER and K. ROBINSON, *Acta Crystallogr.* **20** (1966) 614.
4. P. GUYOT and M. AUDIER, *Phil. Mag.* **B52** (1985) L15.
5. P. GUYOT, *J. Microsc. Spectrosc. Electron.* **10** (1985) 333.
6. V. ELSER, *Phys. Rev.* **B32** (1985) 4892.
7. B. BÜCKLE, *Aluminium-Archiv* (13) (1939) 1.
8. H. W. L. PHILLIPS, *J. Inst. Metals* **69** (1943) 275.
9. G. PHRAGMEN, *J. Inst. Metals.* **77** (1950) 489.
10. J. N. PRATT and G. V. RAYNOR, *Proc. Roy. Soc.* **A203** (1951) 103.
11. M. HILLERT, *CALPHAD* **4** (1980) 1.
12. H. W. L. PHILLIPS, "Annotated equilibrium diagrams of some aluminium alloy systems" (The Institute of Metals, London, 1959).
13. C. J. SIMENSEN, P. FARTUM and A. ANDERSEN, *Fresenius Z. Anal. Chem.* **319** (1984) 286.
14. M. COOPER, *Acta Crystallogr.* **23** (1967) 1106.
15. D. B. WILES and R. A. YOUNG, *J. Appl. Crystallogr.* **14** (1981) 149.
16. C. J. HOWARD, *ibid.* **15** (1982) 615.
17. P. M. SKJERPE, personal communication (1987).
18. K. ROBINSON, *Acta Crystallogr.* **5** (1952) 397.
19. M. A. TAYLOR, *ibid.* **12** (1959) 393.
20. A. DAMJANOVIC and P. J. BLACK, *ibid.* **14** (1961) 987.
21. A. GRIGER, *Powder Diffraction* **2** (1987) 31.
22. V. STEFÁNIAY, A. GRIGER and T. TURMEZEY, *J. Mater. Sci.* **22** (1987) 539.
23. A. GRINGER, V. STEFANIAY and T. TURMEZEY, *Z. Metallkde* **77** (1986) 30.
24. M. E. SEIERSTEN and J. E. TIBBALLS, "An evaluation of the Al–Fe binary system", presented at the 16th CALPHAD meeting, Irsee, West Germany, May 1987.
25. LIU PING and G. DUNLOP, *J. Mater. Sci.* **23** (1988) 1419.

Received 19 April
and accepted 7 September 1988